

Morphological variation of the hemophilic talus

Harriet G. Talbott¹  | Richard A. Wilkins^{2,3}  | Anthony C. Redmond^{2,4}  |
Claire L. Brockett^{1,2,4}  | Marlène Mengoni¹ 

¹Institute of Medical and Biological Engineering, School of Mechanical Engineering, University of Leeds, Leeds, UK

²Leeds Institute of Rheumatology & Musculoskeletal Medicine, Chapel Allerton Hospital, Leeds, UK

³Leeds Haemophilia Comprehensive Care Centre, Leeds Teaching Hospitals NHS trust, Leeds, UK

⁴Centre for Sports, Exercise and Osteoarthritis Versus Arthritis, Nottingham, Oxford, Loughborough, Leeds, UK

Correspondence

Marlène Mengoni, Institute of Medical and Biological Engineering, School of Mechanical Engineering, University of Leeds, Leeds, UK, LS2 9JT.

Email: m.mengoni@leeds.ac.uk

Abstract

Flattening of the trochlear tali is clinically observed as structural and functional changes advance in patients with hemarthropathy of the ankle. However, the degree of this flattening has not yet been quantified, and distribution of the morphological changes across the talus not yet defined. Chronologically sequential MR images of both a hemophilic patient group ($N = 5$) and a single scan from a nondiseased, sex-matched, control group ($N = 11$) were used to take four measurements of the trochlear talus morphology at three locations (medial, central and lateral) along the sagittal plane. Three ratios of interest were defined from these to assess whether the talar dome flattens with disease. The control group MRI measurements were validated against literature data obtained from CT scans or planar X-Rays. The influence of disease on talar morphology was assessed by direct comparison of the hemophilic cases with the control group. The values for all three ratios, in all locations, differed between the control and the hemophilic group. Flattening was indicated in the hemophilic group in the medial and lateral talus, but differences in the central talus were not statistically significant. This work demonstrates that morphological assessment of the talus from MR images is similar to that from CT scans or planar X-Rays. Talar flattening does occur with hemarthropathy, especially at the medial and lateral edges of the joint surface. General flattening of the trochlear talus was confirmed in this small patient sample, however the degree and rate of change is unique to each ankle.

KEYWORDS

hemarthropathy, morphology, MRI, talus

1 | INTRODUCTION

Hemophilia is an X-linked recessive genetic disorder characterized by bleeding within soft tissue and joints (Bolton-Maggs & Pasi, 2003). Musculoskeletal bleeding accounts for up to 90% of all bleed incidence, with the ankle joint the most commonly affected in terms of hemarthrosis and subsequent deterioration of joint health (Stephensen et al., 2009). Recurrent bleeds lead to progressive functional and structural joint changes and eventual chronic ankle

hemarthropathy. Clinical assessment has shown as this joint disease progresses, the talus appears to collapse with changes in geometry, joint space and function. In other diseases affecting the ankle joint, such as clubfoot, talar flattening has been linked with joint incongruity, loss of range of motion and altered gait patterns (Bach et al., 2002; Kolb et al., 2017; Shivers et al., 2020) which pose a significant burden to the patient in terms of pain and disability.

The degenerative and inflammatory responses of Hemophilic Joint Disease (HJD) are identified by radiological classification. In bone,

This is an open access article under the terms of the Creative Commons Attribution License, which permits use, distribution and reproduction in any medium, provided the original work is properly cited.

© 2021 The Authors. *Clinical Anatomy* published by Wiley Periodicals LLC on behalf of American Association of Clinical Anatomists.

subjective phrases such as “Irregularity/erosion of subchondral bone” and “chondral destruction” are used (Lundin et al., 2012), not directly considering clinically observed morphological changes, such as angulation (Jelbert, Vaidya, & Fotiadis, 2009) or talar flattening (Macnicol & Ludlam, 1999). Angulation suggests nonuniform changes across the talar dome occurring with HJD, though this remains unquantified. The differences between nondiseased and HJD bone morphology may implicate mechanical factors in influencing disease progression, as the morphological changes are observed in the region of the joint in articulation with the tibia (Jelbert et al., 2009). It is unknown however, whether these morphological changes are common across the hemophilia population, and whether they alter systematically with progression of HJD. These factors may aid in understanding the etiology of HJD.

Talocrural measurements have been analyzed in nondiseased ankles using radiographs (Fessy, Carret, & Bejui, 1997; Kwon et al., 2014; Stagni, Leardini, Ensini, & Cappello, 2005) and CT images (Claassen et al., 2019; Hayes, Tochigi, & Saltzman, 2006; Kuo et al., 2014; Liu et al., 2020). CT has been the 3D imaging mode of choice as it gives more clearly defined bone boundaries, but is rarely the clinical imaging modality used for HJD patients. These previous studies have investigated factors such as age, sex, body composition and ethnicity on the morphology of the talocrural joint. The literature covers a range of measurements, with four of interest when assessing the morphology of the talar dome: Trochlear Tali Arc Length (TaAL), Talus Height (TaH), Trochlear Tali Length (TaL), Trochlear Tali Radius (TaR) (Figure 1 and Table 1), a combination of which were reported by the seven studies (Claassen et al., 2019; Fessy et al., 1997; Hayes et al., 2006; Kuo et al., 2014; Kwon et al., 2014; Liu et al., 2020; Stagni et al., 2005).

The aims of this study were to assess (a) whether there were systematic morphological differences between the hemophilia tali and nondiseased controls, and (b) whether these changes demonstrated flattening of the talus with HJD progression.

2 | METHODS

2.1 | Patient group and control images

This study used MRI sequences from eight hemophilic ankles and a male control group ($N = 11$) (Local ethical approval MEEC 18-022

following informed consent from the patient or their guardian to use images for research). The eight hemophilic ankles occurred in five patients (three paired ankles, one right ankle and one left ankle). MRI scans were obtained as part of the normal clinical assessment of disease progression. To enable the chronological investigation, each ankle had two or more MRI sequences available (total of 36, two to seven per ankle) taken over several months (6 through 112 months). The patients varied in age at the time of their first scan, from 7 to 39 years. Age was split into three categories for the purpose of this study: pediatric (0–13 years); adolescent (13–18 years); and adult (18 + years). Adolescence was defined separately to pediatrics as bone maturation in the foot is found to complete around 12.5 years (Whitaker, Rousseau, Williams, Rowan, & Hartwig, 2002).

The two groups were matched as closely as possible, based on findings of no significant morphological differences between the right and left talus (Liu et al., 2020), but differences noted by sex (Kuo et al., 2014; Liu et al., 2020). Hemophilia is a sex-linked genetic disorder, hence the patient group was entirely male. The control group was selected from a pre-existing research imaging dataset (Arnold et al., 2020), choosing scans from male volunteers free of ankle joint disease, with images with the correct field of view to include the entire talus.

2.2 | MRI measurements

For each MRI sequence, two dimensional measurements were taken in the sagittal projection of the talus at three locations (medial, lateral and central). A total of 141 images were measured by the first author this study—3x11 control and 3x36 hemophilic images.

Four measurements (Table 1 and Figure 1) were taken from each image using ImageJ (1.52v) (Rasband, 1997-2018; Schneider, Rasband, & Eliceiri, 2012). As this study was longitudinal, natural variability was expected to occur in the overall ankle size. Therefore, to enable comparison between different imaging occasions, three independent ratios were calculated: TaR:TaAL, TaAL:TaL and TaL:TaH (Table 2). Each of these ratios might be expected to show if a flattening effect was occurring with disease. Radii are larger with “flatter” curves, and arc length smaller, therefore TaR:TaAL was expected to increase with flattening. The height of the talus should decrease if a

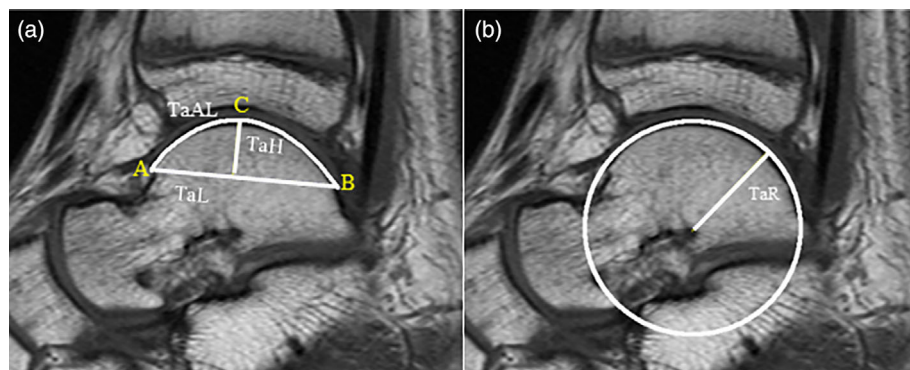


FIGURE 1 Central, sagittal MRI of the talus—annotated with the four key measurements. (a) shows the fitting of the AB arc and chord to produce Trochlear Tali Arc Length (TaAL), Talus Height (TaH) and Trochlear Tali Length (TaL), while (b) shows the fitting of a circle to the talar dome to measure Trochlear Tali Radius (TaR). Medial and lateral measurements were each denoted with m, c or l—that is Lateral Trochlear Tali Length = TaL

TABLE 1 Measurements taken for each image—location of (A), (B) and (C) can be seen in Figure 1

Measurement	Full name	Measurement technique
TaAL (mm)	Trochlear Tali Arc Length	Distance between the most anterior (A), posterior (B) and proximal (C) points in the trochlear tali
TaH (mm)	Talus Height	Height of the trochlear tali, calculated as the distance between point C and the AB line
TaL (mm)	Trochlear Tali Length	Distance between most anterior (A) and posterior (B) points in the trochlear tali—the length of the AB chord.
TaR (mm)	Trochlear Tali Radius	Radius of a circle fitted to the talar dome

flattening was observed, therefore TaL:TaH was also expected to increase. TaAL:TaL is the only variable anticipated to reduce with flattening. If TaAL:TaL had a value of 1 it would suggest a completely flattened trochlear tali.

2.3 | Measurement validation, error analysis and data analysis

The control-group measurements were compared against available data on CT and radiographs to validate the use of MR images. Equivalent measurements from CT (Claassen et al., 2019; Kuo et al., 2014; Liu et al., 2020) and radiographs (Stagni et al., 2005) reporting sex specific measurements, allowing like-for-like comparison against the non-diseased control, were used. Two studies carried out on CT images took measurements across the talus, reporting medial, lateral and central results (Claassen et al., 2019; Kuo et al., 2014), with the ability to compare directly with the radius and arc length measurements of this study. This was not possible for the radiograph study, which reported one maximum value for each length and radius measurement (Stagni et al., 2005). The final CT study was carried out on a 3D model of a talus, where the mean values of height and length were calculated from the maximum measurement for each talus (Liu et al., 2020). For comparison with these latter two studies, the maximum values measured in this work were used.

The difference between the control group measurements and the literature data was assessed using two-tailed Student's *T* Tests. This was performed against all available measurements, except the TaR results of one study (Claassen et al., 2019) that did not agree with previous studies (Kuo et al., 2014; Liu et al., 2020; Stagni et al., 2005).

Measurements were repeated three times for the medial, lateral and central images in the control group to assess for repeatability of selecting the locations of (A), (B) and (C) in Figure 1.

For the first adolescent or adult sequence per ankle, the influence of slice location on measurements and ratios was also analysed. The

four measurements were taken from every slice in the sequence where talar geometry was visible. These measurements were used to assess the difference in ratios between neighbouring slices, and whether this may factor into the results with time.

Three different assessments were made using the three ratios of interest to investigate the effect of HJD on the morphology: comparison of adult data from the hemophilic group to the control group; comparison of individual hemophilic ankle mean to the control group; and changes within each individual hemophilic ankle with time.

In order to age match the two groups when carrying out the first of the three assessments, the hemophilic data excluded 15 images from one patient as the patient was still classified as pediatric for these five sequences.

Statistical analysis was carried out for nonpediatric ratios to assess for normal distribution of results (Shapiro–Wilk test), and equality of variance (Levene test) between the control group and the hemophilia group. Student's *T* Tests were used for five of the nine ratios (TaR:TaALc, TaR:TaALl, TaAL:TaLm, TaAL:TaLl, TaL:TaHl) while Welch's *T* Tests were used for those with unequal variance (TaR:TaALm, TaL:TaHm, TaAL:TaLc and TaL:TaHc).

3 | RESULTS

All measurements for all images are available as open data from an online repository (Talbot et al., 2021).

3.1 | Measurement validation

Both studies that our MRI-derived TaR was assessed against (Kuo et al., 2014; Stagni et al., 2005) showed no difference with respect to measurements derived from CT or radiograph (*p* values between 0.06 and 0.88 for location-specific comparison [Kuo et al., 2014], and 0.82 for comparison of maximum value [Stagni et al., 2005]). Mixed outcomes were found for TaH, where the measurement showed no difference to two values (*p* values of 0.13 [Liu et al., 2020] and 0.82 [Kuo et al., 2014]), comparison of the maximum value only) but yielded statistically significant differences with the third (*p* = 0.006 [Claassen et al., 2019]). This difference was also seen in TaL (*p* = 0.017 [Stagni et al., 2005] and 0.010 [Liu et al., 2020]), and both medial TaAL results (*p* < 0.001 [Claassen et al., 2019; Kuo et al., 2014]). No significant difference from the literature was seen for central TaAL measurements (*p* = 0.39 [Claassen et al., 2019]) and mixed outcomes were obtained for the lateral TaAL measurements (*p* = 0.15 [Kuo et al., 2014] and *p* = 0.005 [Claassen et al., 2019]) (Figure 2).

3.2 | Error evaluation (verification)

In the measurements repeated three times, the main source of error appeared to relate to the precise selection of locations A and B, as not

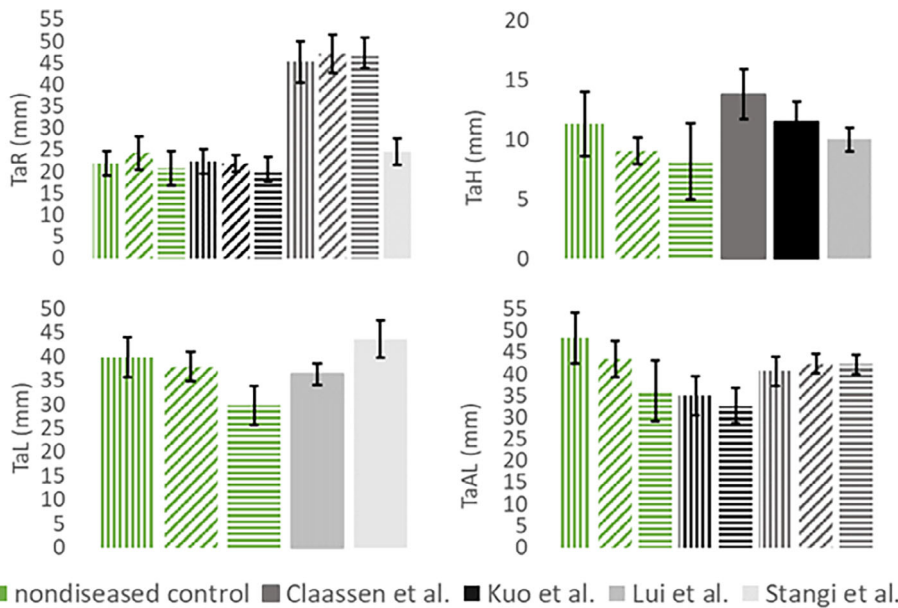


FIGURE 2 Outputs of previous studies compared to the nondiseased control group. Patterns show location across the talus: medial: vertical stripe, central: diagonal stripe, lateral: horizontal stripe, location not specified—block color. Error bars show reported or calculated standard deviation

	TaR:TaAL			TaAL:TaL			TaL:TaH		
	<i>m</i> *	<i>c</i>	<i>l</i>	<i>m</i> *	<i>c</i>	<i>l</i> *	<i>m</i> *	<i>c</i>	<i>l</i> *
Nondiseased	0.46	0.56	0.59	1.21	1.15	1.20	3.64	4.21	4.01
Hemophilia	0.55	0.53	0.61	1.14	1.17	1.14	4.5	4.1	4.75
<i>p</i> values	0.003	0.22	0.31	0.001	0.08	0.004	0.002	0.28	0.05

TABLE 2 Control group and hemophilic (adult) group mean values for each ratio at the three locations (*m*: medial, *c*: central, *l*: lateral), and *p* values from *T* tests (* indicates significant differences)

all images have clear landmarks to define these. However, the measurements were still predominantly within 1% relative difference.

The difference between ratios measured on adjacent slices saw a range of outcomes amongst the hemophilic ankles; TaR:TaAL saw the largest differences between adjacent slices, with values ranging between 1.45% and 103% ($\bar{x} = 15.1\%$), these differences were largest between the most medial and most lateral slices and their respective neighbouring slices. Tali covered by the greatest number of slices consistently saw greater differences at the extremes.

3.3 | Hemophilic group versus nondiseased control group

When comparing the hemophilic ankles as a group to the nondiseased control group, the medial and lateral values for both TaR:TaAL and TaL:TaH were greater in the hemophilic group, whereas TaAL:TaL was smaller (Table 2), all consistent with talar dome flattening. The differences between the hemophilic and nondiseased groups were found to be statistically significant in all ratios in the medial talus, and two of the three ratios in the lateral talus, but not in the central talus (Table 2).

Where the changes were significant between the groups the relative changes in the ratios behaved as expected with a flattening of the talus. The relative changes however, did vary between the ratios. Where the greatest changes occurred, in the medial talus, TaR:TaALm

increased by 20.7% and TaL:TaHm increased by 23.5%, while TaAL:TaLm only decreased by 5.9%.

3.4 | Individual change with time

The eight ankles each responded to HJD differently, demonstrating a different response to the disease over the period images were available for. The change in TaL:TaH for each ankle can be seen in Figure 3 and TaR:TaAL and TaAL:TaL produced similar responses with time. Figure 3 in this section.

These showed more stable morphology in adulthood (Ankle 6: all images, Ankle 1: month 39 to 112), and no clear pattern of morphological response to HJD in pediatrics or adolescents, with responses even differing between paired ankles.

4 | DISCUSSION

This study investigated the influence of HJD on talar morphology and confirmed a nonuniform flattening of the talus with disease, showing nonlinear changes in talar morphology as the disease progresses in time.

Hemophilia is a rare disease, affecting around 1 in 10,000 males in the UK (Stonebraker, Bolton-Maggs, Soucie, Walker, &

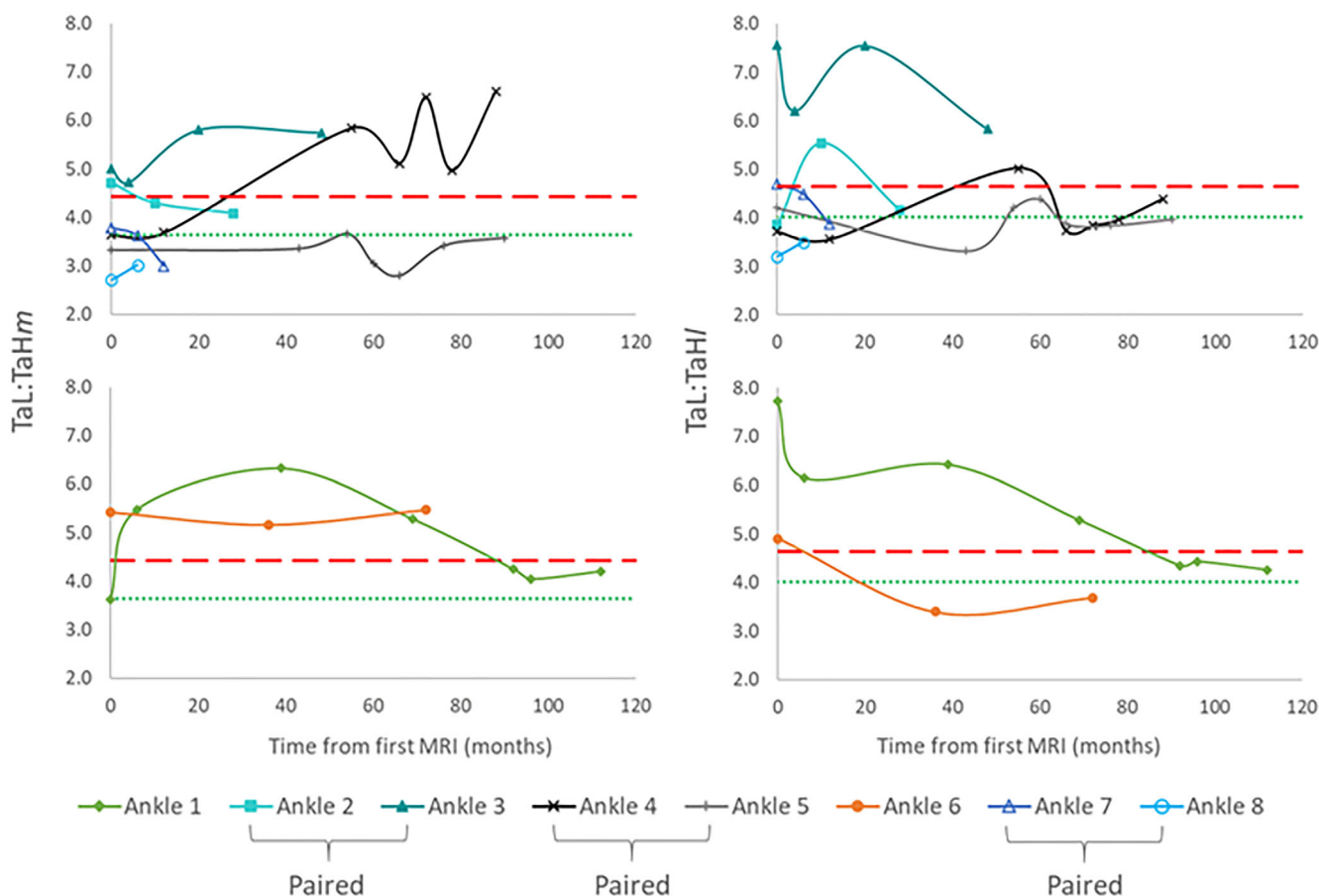


FIGURE 3 Change in TaL:TaHm and TaL:TaHl with time in months. The average trend lines show hemophilic (red dashed) and nondiseased (green dotted) mean values from all eight ankles. The ratios are split into two categories, pediatric/adolescent (first row) and adult (second row). Color-codes relate to the age bracket the patient fell into at the first MRI sequence: grey/black—pediatric; green/blue—adolescent; orange—adult. After ~40 months Ankle 1 moved from adolescent to adult

Brooker, 2010). Of these, approximately 80–90% experience musculoskeletal bleeds (Kasper, 2008; Rodriguez-Merchan, 2010), which occur most commonly in the ankle joint (Stephensen et al., 2009). Due to this, the prevalence of HJD is relatively low compared to other musculoskeletal disorders which is reflected in the number of patient images used in this work despite including all cases available who met the inclusion criteria.

The five patients in the hemophilia group all had at least one affected ankle, with varying degrees of HJD, leading to a total of eight ankles, over 31 points in time included in the results for the hemophilia group. It is known that age and body composition can have small influences on bone geometries (Kuo et al., 2014; Liu et al., 2020), so it was anticipated that a large range of ages (13–45 yo), and mass (45.7–117 kg) would generate a range of measurements. Height could also influence body composition and is highly likely to vary amongst the patients. Ethnicity was another unknown which has been seen to influence measurements (Claassen et al., 2019; Fessy et al., 1997; Hayes et al., 2006; Kuo et al., 2014; Kwon et al., 2014; Liu et al., 2020; Stagni et al., 2005), and would be relevant due to the global prevalence of hemophilia (Stonebraker et al., 2010). Therefore, a novel approach to quantifying the influence

of HJD on talar morphology was required, using morphological ratio rather than direct measurements.

The retrospective nature of the study caused a number of limitations; patients were selected based on the availability of clinical MR images, therefore, the imaging protocol was not controlled. Due to this, the between-slice resolution of some hemophilic sequences were not appropriate for 3D reconstructive models, as carried out in one previous CT study (Kuo et al., 2014). The methods are also limited by the small sample size, which is a reflection of the relatively low prevalence of HJD in the ankle. Statistical shape modelling would have enabled different modes of morphological variation to be assessed, however this typically requires large sample sizes. The benefit of the 2D approach used in this study is the minimal training and resources required for it to be translated into clinical practice.

MRI is not the most appropriate imaging modality for measuring the bone boundaries (Hayashi, Roemer, & Guermazi, 2016), however, is the best medium for assessing arthropathic changes in HJD (Lundin et al., 2012) and is the imaging modality of choice in clinical practice. Comparing MRI derived measures against CT and radiograph measures no differences were found in the trochlear tali radius values,

however, some differences were found in the linear measures of talus height, trochlear talus arc length and trochlear talus length. This could potentially relate to linear measurements being prone to a magnification effect, especially in X-ray derived measures, which will differ across the four studies used for comparison (Claassen et al., 2019; Kuo et al., 2014; Liu et al., 2020; Stagni et al., 2005).

Where measurements were reported across the talus, the central measurement was seen to differ considerably less from the non-diseased control when compared to the medial and lateral measurements (Claassen et al., 2019), this was confirmed by the significant differences seen in the medial and lateral measurements, while there was no significance in the central measurements. Trochlear tali length and talus height were only reported as maximum values in literature, hence it is unclear whether this represents a magnification effect, or due to the location of these maximum values not mapping exactly onto one of the three locations measured in the nondiseased control group. Kuo et al. (2014) did not report a central measurement for trochlear tali arc length to confirm whether it is the definition of bone boundaries in MRI which makes this a more difficult measurement to take, or whether it is the effect of discrepancies in slice location at the medial and lateral extremes.

The differences seen may also occur due to the range of software and methods used for taking the measurements, hence the confirmation against multiple studies with differing approaches to measurement (Mys et al., 2021). Finally, the differences seen between MRI measurements and CT or radiographic measurements ($\bar{x} = 3.13$ mm; 0.17–13.3 mm) were largely lower than the difference between CT and radiographic measurements from the literature ($\bar{x} = 4.61$ mm; 1.48–9.50 mm). Overall, it is likely fair to conclude that the difference in some measurements between MRI and CT or radiographs is as much due to the difference in patient groups as it is in imaging techniques used for the measurements; and that MRI is an adequate modality to evaluate talar morphology.

The verification study indicated a potential error surrounding the subjective manner of selecting the slice to capture the data from, especially in the medial and lateral extremes of the talus. It is not possible to avoid these discrepancies in the hemophilic group, due to the imaging protocol used clinically. The slice thicknesses ranged between 1.5 and 3.6 mm, with the most common protocol giving a slice thickness of 3.3 mm. This limits the number of images to choose from 8 to 11 slices per talus, creating a natural variability. Tali covered by a greater number of slices resulted in greater variability between the most medial and second slice, and the most lateral and penultimate slice. This appeared to occur in ankles where the articular surfaces for the medial malleolus and the articular surface of the lateral process were covered. These marginal slices consequently giving unreasonably small measurements due to the change in talar morphology in these regions. This led to discrepancies in the ratios, however could be accounted for by careful slice selection.

Differences in ratios indicated that the morphology of a male hemophilic talus differs from a disease-free male talus, confirming the predicted nonuniform flattening of the talar dome in the hemophilic population (Jelbert et al., 2009; Macnicol & Ludlam, 1999). When

contrasting the three ratios, it was seen that TaAL:TaL more reliably showed talar flattening across the hemophilic group data.

Changes in morphology were inconsistent across the eight ankles, even those in the three patients with bilateral presentation. Progressive flattening of the talar dome over time was not seen in all eight ankles. However, the methods used in this study have shown that talar flattening can be quantified. The range of individual morphological changes highlight the need to assess each ankle's change over time relative to the initial ratios for that specific ankle. Comparison against mean values of nondiseased or hemophilic populations may be insufficient for assessing degree of disease progression. Now that we have shown flattening of the talus can be quantified in hemophilia, future studies should explore larger samples, perhaps from multiple centres. Linkage with clinical measures of joint health such as the hemophilia joint health score (HJHS) should also be carried out to help clarify the relationship with overall disease progression.

This study showed that morphological changes in each hemophilic ankle are unique. All hemophilic ankles experienced some degree of morphological change, however, the anticipated flattening of the talar dome over time did not occur in all. The degree of change with relation to time varied case by case, therefore, it is unreasonable to extrapolate these results beyond the time period imaged, or suggest that these results would be relevant to all hemophilic ankles.

5 | CONCLUSION

The results indicate that MRI measurements are an adequate substitute for CT or radiograph measurements when evaluating talar morphology. Morphological changes to some degree are seen in ankles with a clinical history of musculoskeletal bleeding. These imply a flattening of the talus which is nonuniform, with a greater influence of the disease on the medial and lateral margins of the talus, and insignificant changes in the centre. This flattening does not progress linearly with the disease—especially in younger patients. Each ankle has an individual response to disease progression, even in those patients with bilateral presentation.

ACKNOWLEDGMENTS

Funding for this research was provided by the EPSRC (grant EP/R513258/1, project 2118904). This work was supported by the National Institute for Health Research (NIHR) Biomedical Research Centre in Leeds and the authors recognise Dr Jill Halstead and Dr John Arnold for their provision of the nondiseased control group data. Thanks are also given to Dr Jill Halstead, who alongside Richard Wilkins identified the disease free ankle joints for use in this research. The authors would finally like to thank both the patients and the control group for their voluntary participation in this research.

ORCID

Harriet G. Talbott  <https://orcid.org/0000-0001-7439-8048>

Richard A. Wilkins  <https://orcid.org/0000-0003-1885-5472>

Anthony C. Redmond  <https://orcid.org/0000-0002-8709-9992>

Claire L. Brockett  <https://orcid.org/0000-0002-6664-7259>

Marlène Mengoni  <https://orcid.org/0000-0003-0986-2769>

REFERENCES

- Arnold, J. B., Halstead, J., Grainger, A. J., Keenan, A. M., Hill, C. L., & Redmond, A. C. (2020). Foot and leg muscle weakness in people with midfoot osteoarthritis. *Arthritis Care Research (Hoboken)*. Epub ahead of print.
- Bach, C. M., Wachter, R., Stöckl, B., Göbel, G., Nogler, M., & Frischhut, B. (2002). Significance of talar distortion for ankle mobility in idiopathic clubfoot. *Clinical Orthopaedics and Related Research*, 398, 196–202.
- Bolton-Maggs, P. H. B., & Pasi, K. J. (2003). Haemophilias A and B. *The Lancet*, 361, 1801–1809.
- Claassen, L., Luedtke, P., Yao, D., Ettinger, S., Daniilidis, K., Nowakowski, A. M., Mueller-Gerbl, M., Stukenborg-Colsman, C., & Plaass, C. (2019). Ankle morphometry based on computerized tomography. *Foot and Ankle Surgery*, 25, 674–678.
- Fessy, M., Carret, J., & Bejui, J. (1997). Morphometry of the talocrural joint. *Surgical and Radiologic Anatomy*, 19, 299–302.
- Hayashi, D., Roemer, F. W., & Guermazi, A. (2016). Imaging for osteoarthritis. *Annals of Physical and Rehabilitation Medicine*, 59, 161–169.
- Hayes, A., Tochigi, Y., & Saltzman, C. (2006). Ankle morphometry on 3D-CT images. *The Iowa Orthopaedic Journal*, 26, 1–4.
- Jelbert, A., Vaidya, S., & Fotiadis, N. (2009). Imaging and staging of hemophilic arthropathy. *Clinical Radiology*, 64, 1119–1128.
- Kasper, C. (2008). *Treatment of hemophilia: hereditary plasma clotting factor disorders and their management*. World Federation of Haemophilia.
- Kolb, A., Willegger, M., Schuh, R., Kaider, A., Chiari, C., & Windhager, R. (2017). The impact of different types of talus deformation after treatment of clubfeet. *International Orthopaedics*, 41, 93–99.
- Kuo, C.-C., Lu, H.-L., Leardini, A., Lu, T.-W., Kuo, M.-Y., & Hsu, H.-C. (2014). Three-dimensional computer graphics-based ankle morphometry with computerized tomography for total ankle replacement design and positioning. *Clinical Anatomy*, 27, 659–668.
- Kwon, D. G., Sung, K. H., Chung, C. Y., Park, M. S., Lee, S. H., Kim, T. W., Lee, J. H., Kim, T. G., & Lee, K. M. (2014). Preliminary findings of morphometric analysis of ankle joint in Korean population. *The Journal of Foot and Ankle Surgery*, 53, 3–7.
- Liu, Y., Han, Q., Yin, W., Wang, C., Chen, B., Wu, N., Zhang, A., & Wang, J. (2020). Sex determination from talus in Chinese population by three-dimensional measurement approach. *Legal Medicine*, 44, 101647.
- Lundin, B., Manco-Johnson, M. L., Ignas, D. M., Moineddin, R., Blanchette, V. S., Dunn, A. L., Gibikote, S. V., Keshava, S. N., Ljung, R., Manco-Johnson, M. J., Miller, S. F., Rivard, G. E., & Doria, A. S. (2012). An MRI scale for assessment of hemophilic arthropathy from the International Prophylaxis Study Group. *Haemophilia*, 18, 962–970.
- Macnicol, M. F., & Ludlam, C. A. (1999). Does avascular necrosis cause collapse of the dome of the talus in severe hemophilia? *Haemophilia*, 5, 139–142.
- Mys, K., Varga, P., Stockmans, F., Gueorguiev, B., Wyers, C. E., van den Bergh, J. P. W., & van Lenthe, G. H. (2021). Quantification of 3D microstructural parameters of trabecular bone is affected by the analysis software. *Bone*, 142, 115653.
- Rasband, W. S. (1997–2018). *ImageJ*. U.S. National Institutes of Health.
- Rodríguez-Merchan, E. C. (2010). Musculoskeletal complications of hemophilia. *HSS Journal*, 6, 37–42.
- Schneider, C. A., Rasband, W. S., & Eliceiri, K. W. (2012). NIH image to ImageJ: 25 years of image analysis. *Nature Methods*, 9, 671–675.
- Shivers, C., Siebert, M., Zide, J. R., Tulchin-Francis, K., Stevens, W., Borchard, J., Riccio, A., & Zide, J. R. (2020). Functional implications of the flat-topped talus following treatment of idiopathic clubfoot deformity. *Foot & Ankle Orthopaedics*, 5, 2473011420S2473000441.
- Stagni, R., Leardini, A., Ensini, A., & Cappello, A. (2005). Ankle morphometry evaluated using a new semi-automated technique based on X-ray pictures. *Clinical biomechanics*, 20, 307–311.
- Stephensen, D., Tait, R. C., Brodie, N., Collins, P., Cheal, R., Keeling, D., Melton, K., Dolan, G., Haye, H., Hayman, E., & Winter, M. (2009). Changing patterns of bleeding in patients with severe hemophilia A. *Haemophilia*, 15, 1210–1214.
- Stonebraker, J. S., Bolton-Maggs, P. H., Soucie, J. M., Walker, I., & Brooker, M. (2010). A study of variations in the reported hemophilia A prevalence around the world. *Haemophilia*, 16, 20–32.
- Talbott, H. G., Wilkins, R. A., Redmond, A. C., Brockett, C. L., & Mengoni, M. (2021). Changes in Morphology of the Haemophilic Talus: data derived from MR Images. [Dataset]. <https://doi.org/10.5518/983>.
- Whitaker, J. M., Rousseau, L., Williams, T., Rowan, R. A., & Hartwig, W. C. (2002). Scoring system for estimating age in the foot skeleton. *American Journal of Physical Anthropology*, 118, 385–392.

How to cite this article: Talbott, H. G., Wilkins, R. A., Redmond, A. C., Brockett, C. L., & Mengoni, M. (2021). Morphological variation of the hemophilic talus. *Clinical Anatomy*, 34(6), 941–947. <https://doi.org/10.1002/ca.23757>